

Assimilation of polar orbiting satellite data in the JMA operational NWP systems

Kozo Okamoto*, Hiromi Owada, Yoshiaki Sato, Masaya Takahashi and Eiji Ozawa

Numerical Prediction Division (NPD) / Japan Meteorological Agency (JMA)

Abstract

The Japan Meteorological Agency (JMA) uses various satellite data in its operational data assimilation systems (DASs) for numerical weather prediction (NWP). The data include radiances and retrievals from ATOVS onboard NOAA and Aqua satellites, and microwave radiometers (MWRs) onboard TRMM, Aqua and DMSP satellites, ocean surface wind vectors from microwave scatterometer on QuikSCAT, vertical refractivity profiles from Global Positioning System - Radio Occultation (GPS-RO), atmospheric motion vectors (AMV) from imagers onboard Aqua, Terra and geostationary satellites, and clear sky radiances from MTSAT-1R imager. They are all inevitable to keep and improve the accuracy of NWP, and we continue to improve the usage and introduce new satellite data. This paper describes the current usage of data from polar orbiting satellites and their impacts on analyses and forecasts mainly in the global DAS.

1. DATA ASSIMILATION SYSTEM (DAS) OF JMA

JMA operates three deterministic NWP models: the Global Spectral Model (GSM), the Regional Spectral Model (RSM) and the Meso-Scale Model (MSM). Their initial conditions are provided by global DAS (GDAS), regional DAS (RDAS) and meso-scale DAS (MDAS), respectively (Japan Meteorological Agency 2007). They are all based on an incremental four dimensional variational (4D-Var) method with horizontal resolutions of 60 km (120 km), 20 km (40 km), and 10 km (20 km) for outer (inner) loop minimization, respectively. Their vertical resolution is 40, 40 and 50, respectively. GSM will be substantially upgraded in terms of the increase of horizontal and vertical resolution to 20 km and 60 layers, and GDAS will also have finer resolution of 20km (80km) in November 2007. Then, RSM and RDAS will be merged into the new GSM and GDAS. The meso-scale 4D-Var will be also upgraded to a non-hydrostatic 4D-Var system (Honda et al. 2005) from the current hydrostatic 4D-Var system in early 2008.

Table 1 is a list of satellite data operationally assimilated in GDAS and MDAS as of September 2007. GDAS uses various satellite data in advanced methods including a direct radiance assimilation. In contrast, MDAS still uses some conventional satellite data such as temperature retrievals from ATOVS and has not yet been assimilating some new data such as Global Positioning System - Radio Occultation (GPS-RO) and clear sky radiances from MTSAT because of the limited computer resource due to its tight operational schedule. The advanced methods and new data that GDAS already adopted will be also used in MDAS if they ensure positive impacts for the computational burdens. Hereafter the paper focuses on the recent development of satellite data assimilation of sounders, scatterometers and GPS-RO in GDAS. Other developments can be found in Okamoto et al. (2006).

type	Variables assimilated	Satellite	Sensor	Assimilation system
Sounder	Radiance	NOAA15~18, Aqua	AMSU-A,-B,MHS	GDAS
	Temperature	NOAA15~18	AMSU-A,-B,MHS,HIRS	MDAS
Microwave radiometer	Radiance	DMSP-F13,14, TRMM, Aqua	SSMI, TMI, AMSR-E	GDAS
	Total column water vapor, Rain-rate			MDAS
Scatterometer	Ocean wind vector	QuikSCAT	SeaWinds	GDAS, MDAS
GPS-RO	Refractivity	CHAMP	BlackJack	GDAS
Imager	Atmospheric motion wind	Aqua, Terra	MODIS	GDAS
		MTSAT-1R, GOES-11,12, METEOSAT-7,9	JAMI, IMAGER, SEVIRI	GDAS, MDAS
	Clear sky radiance	MTSAT-1R	JAMI	GDAS

Table 1: Satellites, instruments and variables operationally assimilated in the JMA global and meso-scale assimilation systems as of September 2007.

2. SOUNDER

Less cloud/rain affected radiances of AMSU-A, AMSU-B, and MHS are used in GDAS. Some of AMSU-A channels 4-13 and AMSU-B/MHS channels 3-5 are chosen according to the cloud/rain and surface conditions such as ocean, land, sea-ice and coast. A fast radiative transfer calculation required for the radiance assimilation is performed using RTTOV version 7 (Saunders et al. 2002). A thinning procedure selects a sounding profile closer to the center time of each time slot and the center of a thinning grid box. The size of the thinning box is set to 250x250 km² for AMSU-A and 180x180 km² for AMSU-B and MHS. A gross error check rejects the data when observed-minus-background (O-B) exceeds three times the observation error (σ_{obs}) which is predefined for each channel based on standard deviation (STD) of bias-corrected O-B. The background radiance is calculated from first-guess field. Observation biases are removed using a two-step procedure: First, a scan-dependent bias correction (ScanBC) removes a large portion of biases by subtracting precalculated O-B average at each scan position. Second, the residual bias is removed by a variational bias correction (VarBC, Derber and Wu 1998; Dee 2004). VarBC calculates biases to be corrected using a linear equation with several air-mass-related predictors and their coefficients are obtained as analysis variables of 4D-Var main analysis so that they are consistent with background and other observations. In August 2006, we made several improvements in ATOVS pre-processings (quality control and thinning method), recalculated the ScanBC dataset and reevaluated observation errors. These modification yielded obvious positive impacts especially in short-range forecast in the Southern Hemisphere (Okamoto et al. 2006).

AMSU-A, -B and MHS radiances from the Asia-Pacific ATOVS Retransmission Services (AP-RARS) and the EUMETSAT Advanced Retransmission Service (EARS) were added in the GDAS in February 2007 and August 2007, respectively. AP-RARS ATOVS data from 10 stations in Australia, China, Korea and Japan, including Japan's Syowa Station on the Antarctica, are assimilated. The use of these early delivery data from AP-RARS and EARS in early analysis of GDAS makes the analysis closer to cycle analysis of GDAS. The early analysis generating forecast products cannot have enough time (2h25m in GDAS) to wait for satellite data coming in. In contrast, the cycle analysis assimilates more satellite data due to longer data cut-off time length (5h35m for 00 and 12 UTC and 11h35m for 06

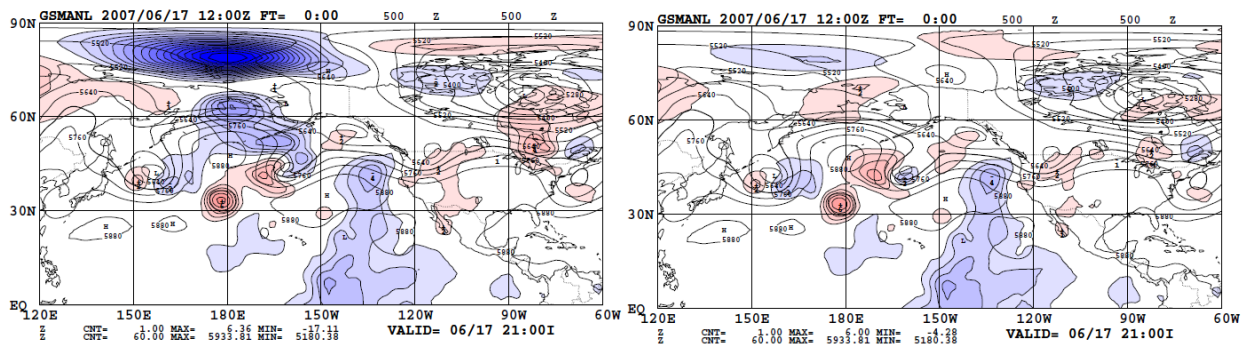


Figure 1: Difference between early analysis and cycle analysis for geopotential height at 500 hPa (Z500) in EXP-NORARS (left) and EXP-EARS (right) at 12UTC on 17 June 2007. Blue (red) shades depict positive (negative) value of the difference and contours indicate 500Z.

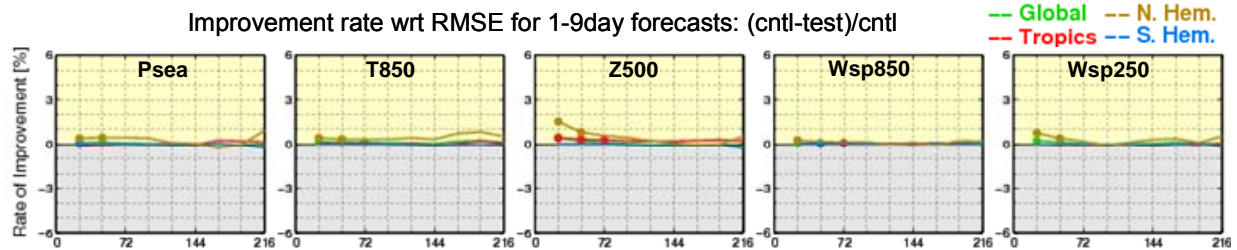


Figure 2: Forecast improvement rate (error reduction rate) with respect to root mean square forecast error (RMSFE) in terms of sea surface pressure (Psea), temperature at 850 hPa (T850), Z500, wind speed at 850 hPa and 250 hPa (Wsp850 and Wsp250). The improvement rate is RMSFE difference of an EXP-NORARS (cntl) from an EXP-EARS (test) normalized by cntl RMSFE, being positive for smaller RMSFE in test. It is calculated for the Northern Hemisphere (brown), Tropics (red), Southern Hemisphere (blue) and the globe (green), and dots on lines represent statistical significance.

and 18 UTC in GDAS), being generally more accurate than the early analysis. In order to assess impacts of AP-RARS and EARS individually, three one-month early analysis experiments were carried out: “EXP-NORARS” experiment where operational data configuration then were used, “EXP-APRARS” experiment where AP-RARS ATOVS data were added to EXP-NORARS, and “EXP-EARS” experiment where EARS ATOVS data were added to EXP-NORARS. EXP-APRARS showed a better fit to cycle analysis with respect to the geopotential height mostly in the stratosphere around RARS stations than in EXP-NORARS. Meanwhile, EXP-EARS showed much better agreement with the cycle analysis for the 500 hPa geopotential height (Z500) in the mid- and high-latitudes of the Northern Hemisphere (Fig.1) and better forecasts in the Northern Hemisphere and Tropics than EXP-NORARS (Fig. 2). Greater impacts of EARS were probably yielded by the fact that the number of EARS ATOVS data available was generally three times more than that of AP-RARS ATOVS data.

JMA started receiving level1B data of AMSU-A and MHS on Metop from EUMETSAT via GTS on 7 February 2007. The stability and timeliness of the data dissemination, which are essential for operational NWP system, have been entirely satisfactory. Cycle experiments assimilating these data showed substantial positive impacts on forecasts at day 1 to day 3 despite of already using four NOAA satellites (NOAA15-18) and Aqua satellites (Fig.3).

The assimilation of the hyperspectral infrared sounder AIRS onboard Aqua is being developed. Initial target is clear radiances of 76 channels over the ocean. The channel selection out of 324 channels we

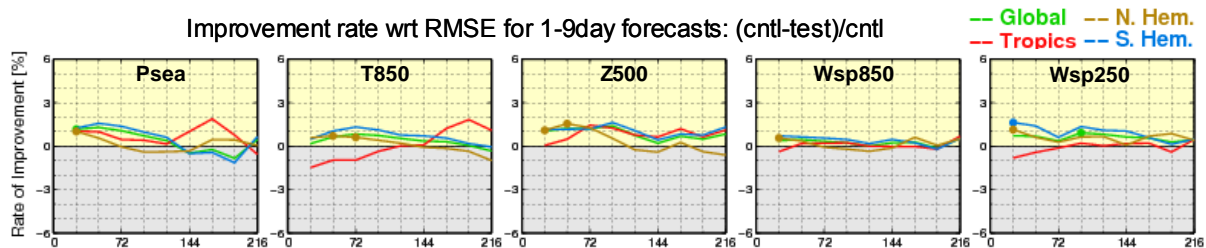


Figure 3: Forecast improvement rate for the experiment using Metop (test) against the experiment using no Metop (cntl).

are receiving is performed using an entropy reduction method (Rodgers 2000), and cloud contaminated measurements are identified based on McNally and Watts (2003). The bias correction scheme adopts the same method as ATOVS except VarBC predictors. Initial results of a cycle experiment provided the increase in analysis biases for the temperature and moisture and unsatisfactory forecast scores for the representative variables such as geopotential height. This degradation might be caused by treatment of water vapor channels that have large background departures and an improper bias correction. Moreover, as the effect of AIRS seemed to be much larger than it should be (cost function value of AIRS radiance is too large compared with those of other observations), the reevaluation of observation errors and channel selection taking into account inter-channel correlation may be needed.

3. SCATTEROMETER

The key issue of the assimilation of ocean surface wind vectors derived from scatterometers is how to treat with wind vector uncertainties. Only one wind vector out of two to four candidates at each measurement pixel is selected in both GDAS and MDAS. The selection is made by an ambiguity removal procedure which keeps the vector consistent with adjacent vectors using a median filter technique, followed by a group QC procedure where grouped vectors are compared with first-guesses with respect to their wind directions. In addition to these procedures, several data-screening procedures are performed which remove the data contaminated by rain or ice-sea and the data with $|O-B|$ greater than 30 % of the background wind speed. The data passing all these procedures are thinned to 100 km distance and assimilated in 4D-Var.

Ohhashi (2004) showed that QuikScat improved forecast skills for the Z500 in the Northern

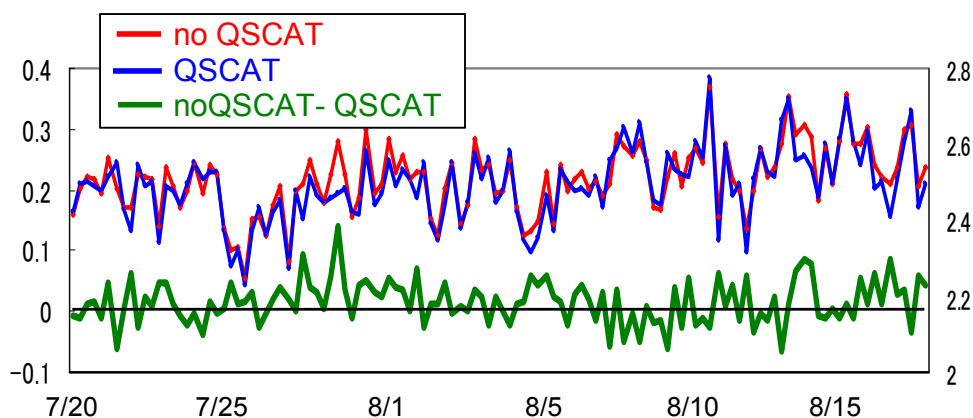


Figure 4: RMSE of ocean wind speed [m/s] between first-guess and buoys and ships from 20 July though 20 August, 2006. The blue (red) line indicates RMSE in the right axis when QuikSCAT is used (not used), and the green line the RMSE difference, which is positive when adding QuikSCAT reduces the RMSE, in the left axis.

Hemisphere, 850Z in the Tropics, and typhoon track in the previous GDAS based on 3D-Var method. Recently we have reevaluated its impact in the current operational GDAS based on 4D-Var method. The assimilation of QuikSCAT improved the fit of first-guess to in-situ ocean surface wind measurements (Fig. 4). It also improved forecast skills of RMSE for the surface pressure and Z500 in the Tropics and Southern Hemisphere. Typhoon track forecasts were also improved in many cases although they might not be statistically significant because only six typhoons occurred during the experiment period (20 July through 10 September 2006).

4. GPS-RO

In order to exploit temperature and moisture information along the ray-path between GPS satellites and low earth orbit (LEO) satellites that receive GPS radio signals, refractivity data are assimilated at tangent points where ray-paths are closest to the center of Earth. Assimilating another possible data type of a bending angle, which has the advantage of small biases, is not adopted because the refractivity assimilation gave comparable skills with the bending angle assimilation through cycle experiments while the latter needs much more computational costs. The refractivity data up to an altitude of 5 km, which generally have large biases, are removed. The data above 5 km are bias-corrected and assimilated when $|O-B| < 2 \cdot \sigma$ with respect to refractivity, where σ is precalculated O-B STD and varies with the TP altitude. The bias correction is performed using a linear regression with predictors of observation latitude, refractivity and altitude, and their coefficients are determined and updated by a Kalman Filter technique in every analysis pre-processing. Finally the data are selected such that their vertical spacing is 2 km, and are assimilated in the 4D-Var analysis.

Cycle experiments using the refractivity data from the CHAMP satellite (Wickert et al. 2000) were conducted for August 2004 and January 2005. Although only 50 to 80 refractivity data are assimilated in each analysis, small but positive impacts on forecasts were obtained. Figure 5 shows the difference of RMSFE verified against radiosondes observations in terms of temperature for 1-day through 9-day forecasts between the experiment using CHAMP refractivity data (EXP_RO) and the experiment not using them (EXP_NORO). The RMSFE reduction is found at almost all forecast days and levels especially around 300 hPa.

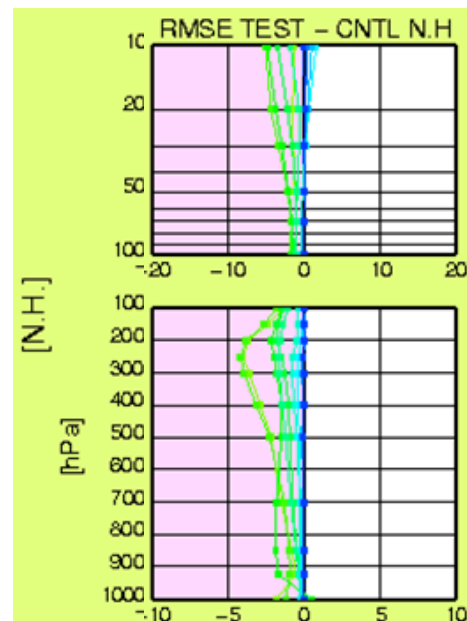


Figure 5: The difference of RMSFE of temperature [K] verified against radiosondes in the Northern Hemisphere. EXP-RO minus EXP-NORO are calculated from 1-day to 9-day forecast and plotted at each forecast day in blue to light-green lines.

5. SUMMARY AND PLANS

JMA has been vigorously developing the satellite data assimilation. We have made several changes in the introduction of new data (MWR radiances in May 2006, GPS-RO in March 2007, clear sky radiances of MTSAT-1R imager in June 2007), improvement of processings (ATOVS radiances in

August 2006 and atmospheric motion vectors from geostationary satellites in October 2006), and the addition of data (AP-RARS and EARS ATOVS in February and August 2007).

Work is proceeding to assimilate new data such as various meteorological instruments on Metop and SSMIS on DMSP. Furthermore the enhancement of the current usage is underway. For instance, all ambiguous wind vectors, instead of the sole wind vector surviving the ambiguity removal procedure in the current processing, will be assimilated based on Stoffelen and Anderson (1997). The assimilation of cloud/rain-affected radiances, in addition to clear/less cloud-affected radiance, is under development. To suit finer horizontal and vertical resolution in new GDAS, horizontal and vertical spacing should be reevaluated in an observation thinning or averaging procedure and a vertical interpolation method should be revised. Assimilating radiances of sounders and MWRs, instead of retrieval products, in MDAS is also under development.

REFERENCES

Dee, D. P. (2004) Variational bias correction of radiance data in the ECMWF system. Proceedings of the ECMWF workshop on assimilation of high spectral resolution sounders in NWP. Reading, UK. 28 June - 1 July 2004.

Derber, J. C. and Wu, W.-S. (1998) The use of TOVS cloud-cleared radiances in the NCEP SSI analysis system. *Mon. Wea. Rev.*, **126**, pp 2287-2299.

Honda, Y., Nishijima, M., Koizumi, K., Ohta, Y., Tamiya, K., Kawabata, T. and Tsuyuki, T. (2005) A pre-operational variational data assimilation system for a non-hydrostatic model at the Japan Meteorological Agency: Formulation and preliminary results. *Quart. J. Roy. Meteor. Soc.*, **131**, pp 3465-3475.

Japan Meteorological Agency (2007) Outline of the operational numerical weather prediction at the Japan Meteorological Agency. Appendix to WMO numerical weather prediction progress report. available on <http://www.jma.go.jp/jma/jma-eng/jma-center/nwp/outline-nwp/index.htm>

McNally, A. P. and Watts, P. D. (2003) A cloud detection algorithm for high-spectral-resolution infrared sounders. *Quart. J. Roy. Meteor. Soc.*, **129**, pp 3411-3423.

Ohhashi, Y. (2004) Assimilation of QuikSCAT/SeaWinds Ocean Surface Wind Data into the JMA Global Data Assimilation System. RSMC Tokyo Typhoon Center Technical Review, No. 7, Japan Meteorological Agency, pp 22-27. available on <http://www.jma.go.jp/jma/jma-eng/jma-center/rsmc-hp-pub-eg/techrev.htm>

Okamoto, K., Owada, H., Sato, Y. and Ishibashi, T. (2006) Use of satellite radiances in the global assimilation system at JMA. Proceedings of the 15th International TOVS Study Conference, Maratea, Italy, 4-10 October 2006.

Rodgers, C. D. (2000) Inverse methods for atmospheric sounding: Theory and Practice, World Scientific, 238pp.

Saunders, R., Brunel, P., Chevallier, F., Deblonde, G., English, S., Matricardi, M. and Rayer, P. (2002) RTTOV-7 science and validation report. available on <http://www.metoffice.com/research/interproj/>

nwpsaf/rtm/rttov7_svr.pdf

Stoffelen, A. and Anderson, D. (1997) Ambiguity removal and assimilation of scatterometer data. *Quart. J. Roy. Meteor. Soc.*, **123**, pp 491-518.

Wickert, J., Reigber, C., Beyerle, G., König, R., Marquardt, C., Schmidt, T., Grunwaldt, L., Galas, R., Meehan, T. K., Melbourne, W. G. and Hoche K. (2000) Atmosphere sounding by GPS radio occultation: First results from CHAMP. *Geophys. Res.*, **28**, pp 3263-3266.